HETEROCYCLES, Vol. 94, No. 4, 2017, pp. 676 - 690. © 2017 The Japan Institute of Heterocyclic Chemistry
Received, 14th January, 2017, Accepted, 21st March, 2017, Published online, 28th March, 2017
DOI: 10.3987/COM-17-13651

SYNTHESIS AND STRUCTURAL CHARACTERIZATION OF DIAZULENYLBORINIC ACID

Toshihiro Murafuji,[a,b,c]* Kohhei Shintaku,[b] Kouhei Nagao,[c] Yuji Mikata,[d] Katsuya Ishiguro,[a,c] and Shin Kamijo[a,c]

[a] Graduate School of Sciences and Technology for Innovation, Yamaguchi University, Yamaguchi 753-8512, Japan. E-mail: murafuji@yamaguchi-u.ac.jp

[b] Graduate School of Medicine, Yamaguchi University, Yamaguchi 753-8512, Japan

[c] Department of Chemistry, Faculty of Science, Yamaguchi University, Yamaguchi 753-8512, Japan

[d] Department of Chemistry, Biology, and Environmental Science, Faculty of Science, Nara Women's University, Nara 630-8506, Japan

Abstract – Diazulenylborinic acid **1** was synthesized by the reaction of 1,3-dibromoazulen-2-yllithium (**2**) with 1,3-dibromoazulen-2-ylboronic acid ethylene glycol ester (**7d**). The X-Ray crystallographic study of **1** revealed that it forms a dimeric structure through intermolecular hydrogen bonding between the hydroxyl groups. To obtain the tetracoordinate borinate derivative from **1**, the attempted esterification of **1** with *N*,*N*-dimethylethanolamine did not give corresponding borinate **8** but resulted in the unexpected protodeboronation to give parent 1,3-dibromoazulene (**4**). The ^{13}C and ^{11}B NMR studies of **1** in the presence of Et_3N revealed the change in the π-polarization of the azulenyl group accompanied by the change in the geometry of the boron to a tetracoordinate structure.

INTRODUCTION

Azulene, a nonalternant hydrocarbon and isomer of alternant naphthalene, is physicochemically characterized by high electron affinity, low ionization potential, and low aromatic energy, together with the dipole moment vector whose negative end is toward its five-membered ring. Construction of π-electron systems based on nonalternant azulene has been attracting increasing interest.[1] Because the resonance stabilization of nonalternant conjugation is smaller than that of alternant conjugation, slight

structural modification of nonalternant molecules induces a significant change in the properties.[2] Thus, we have reported the introduction of a nonalternant 1,3-dihaloazulen-2-yl group on a pnictogen center (Scheme 1).[3] Oxidation of the pnictogen centers markedly increases the π-polarization in the azulenyl group, which is detected in solution by a color change as well as by changes in the ^{13}C NMR spectroscopic characteristics.

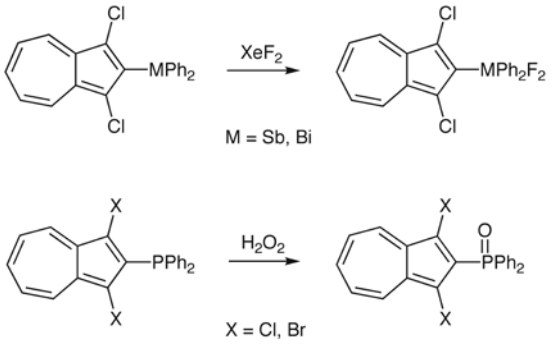

Scheme 1. Oxidation of azulenylpnictogens

It is important to understand how the nonalternant ligand affects the structure and properties of organometallic compounds depending on the nature of the metal center and its valency. Despite the unique electronic structure of the nonalternant conjugation, studies of the properties of organometallics bearing a nonalternant azulenyl group have been very limited.[4] Herein, we report the synthesis, reaction and structural characterization of bis(1,3-dibromoazulen-2-yl)borinic acid (**1**), a boron analog of our previously reported azulenyl pnictogen derivatives. Recently, there have been a number of diarylborinic acids reported involving their unique reactivities and utilities depending on the aryl groups.[5-9] Although diarylborinic acids are unstable under ambient conditions and easily undergo oxidation to give phenols and phenylboronic acids,[6,7,10] **1** is stable under ambient conditions. We performed X-ray structure analysis of **1**. To the best of our knowledge, the X-ray crystallographic studies of diarylborinic acids have been very limited.[11-15]

RESULTS AND DISCUSSION

Synthesis and reaction of 1: Our initial efforts were aimed at identifying conditions for the synthesis of **1**. Most synthetic methods for diarylborinic acids are based on the reaction of organolithiums or Grignard reagents with boron based electrophiles.[16] Hence, we planned to use azulenyllithium **2** or azulenylmagnesium bromide **3** (Scheme 2). We have established the methodology to generate **2** and **3** from **4** and **5**, respectively.[17] Azulenyllithium **2** is less stable above –30 °C whereas Grignard reagent **3** is stable at ambient temperature. 1,3-Dibromoazulene (**4**) was synthesized by the bromination of azulene with NBS. 1,3-Dibromo-2-iodoazulene (**5**) was obtained by the lithiation of **4** followed by the trapping of **2** with iodine.

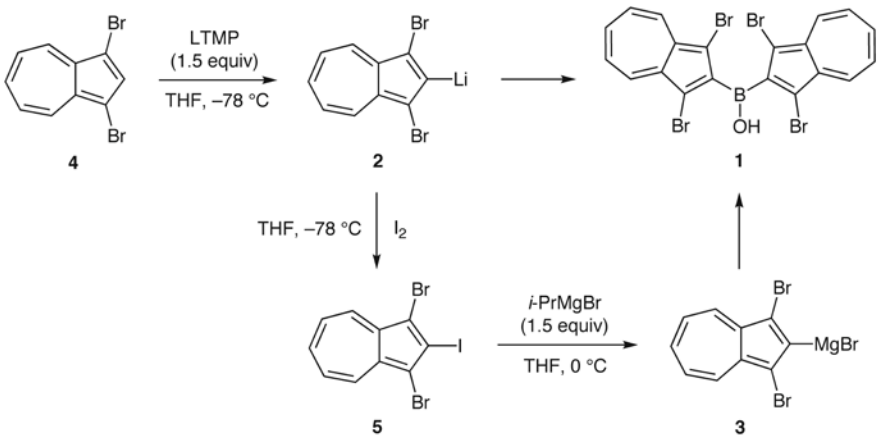

Scheme 2. Synthetic plan for **1** from **2** and **3**

The reactions of **2** or **3** with boron electrophiles are summarized in Table 1. Initially, **2** was generated from **4** by treatment with lithium 2,2,6,6-tetramethylpiperidide (LTMP) (1.5 equiv) in THF at –78 °C. Addition of BF_3•OEt_2 (1.0 equiv) at this temperature to the green solution containing **2** gave a dark brown solution (entry 1). Workup with aqueous HCl at room temperature followed by extraction and subsequent concentration of the extracts gave a residue containing brown intractable substances. Purification of the residue by chromatography (silica gel) gave **6** in only 12% yield along with a large amount of recovered **4** (56%).

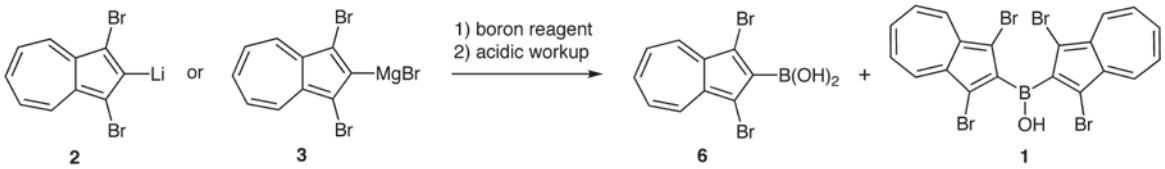

Table 1. Reaction of **2** or **3** with boron electrophiles

entry	**2** or **3**	boron reagent (equiv)	solvent	temp (°C)	time (h)	yield (%)		recovery (%)
						6	**1**	**4**
1	**2**	BF_3•OEt_2 (1.00)	THF	–78	1	12	0	56
2	**2**	BF_3•OEt_2 (0.33)	THF	–78	1	12	0	25
3	**2**	$B(OMe)_3$ (1.00)	THF	–78	1	68	0	0
4	**2**	$B(OMe)_3$ (0.33)	THF	–78	1	76	0	8
5	**3**	BF_3•OEt_2 (0.33)	THF	rt	72	54	8	40
6	**3**	BF_3•OEt_2 (0.50)	THF	reflux	24	24	5	0
7	**3**	BF_3•OEt_2 (0.15)	toluene	reflux	4	29	18	15

The yields of **6** and **1** are based on the boron reagent.

The recovery of **4** in entries 5–7 is based on **5**.

In entry 2, a similar reaction of **2** with BF_3•OEt_2 (0.33 equiv) resulted in the formation of **6** in 12% yield together with recovered **4** (25%). Using trimethyl borate instead of BF_3•OEt_2 also resulted in the formation of **6** (entries 3 and 4). Next, we generated **3** from **5** by a halogen–metal exchange reaction and

tried the reaction with BF_3•OEt_2. In entry 5, when **3** was allowed to react with BF_3•OEt_2 (0.33 equiv), we found that **1** was formed in 8% yield as a minor product as well as **6** (54%) along with recovered **4** (40%). A similar reaction using BF_3•OEt_2 (0.50 equiv) under reflux slightly decreased the yield of **1** (entry 6). When toluene was used as a solvent after removal of THF by distillation and the reaction of **3** with BF_3•OEt_2 (0.15 equiv) was conducted under reflux, the yield of **1** was improved to 18%.

To increase the yield of **1** by reducing the formation of **6**, we focused on entry 3. Because the yield of **6** (68%) was higher in Table 1, we envisaged that replacing trimethyl borate in the reaction in entry 3 with boronic acid esters derived from **6** would afford **1** through the nucleophilic attack of **2** at the boron in these esters. Diarylborinic acids bearing different aryl groups have been synthesized from arylboronic acid ester and aryllithium.[18] On the basis of this idea, we synthesized various cyclic boronic esters **7** (Scheme 3).[19,20] The ring closure of **6** with diols was complete within 3 h at room temperature to give corresponding **7** in high yields. Only in the case of **7b**, the reaction was very slow (42 h). This may be attributed to the lower nucleophilicity of the hydroxyl oxygen due to the conjugation with the benzene ring.[19] The ^{11}B NMR spectra of **7** showed that the signal due to the boron atom appeared around δ 30 ppm except for **7c**. The boron signal of **7c** was found more upfield (δ 11.4 ppm). This is consistent with the presence of the intramolecular coordination with the nitrogen atom in **7c**. Compound **7c** gradually underwent protodeboronation[21] in the solid state at room temperature to give **4** quantitatively. No such deboronation was observed in other derivatives of **7**. Compounds **7a** and **7b** were possible to purify by chromatography (silica gel), but **7d-f** underwent hydrolysis to form **6** quantitatively.

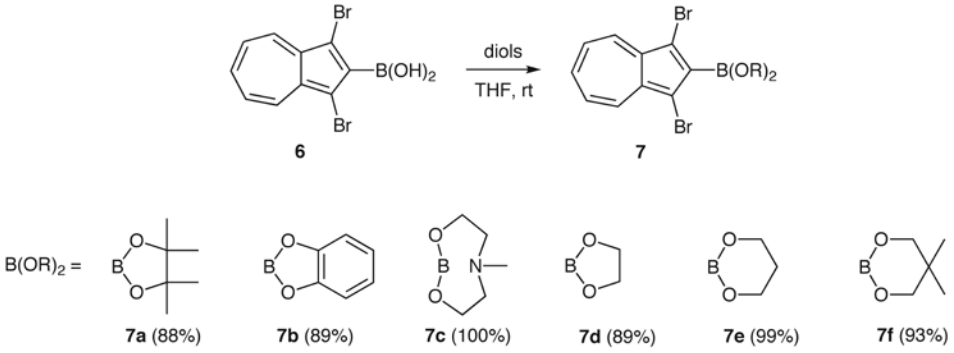

Scheme 3. Conversion of **6** into **7**

Next, we examined the reaction of **7** with **2** and found that the yield of **1** depended on the ring size and steric effect of the boronic ester moiety (Table 2). In entry 1, the yield of **1** was poor because four methyl substituents block the nucleophilic attack at the boron. The poor yield of **1** in entry 2 was attributed to the rigid cyclic boronate moiety around the boron atom since most of **7b** was recovered (82%) without hydrolysis. The intramolecular boron–nitrogen coordination in **7c** completely suppressed the formation of **1** (entry 3). Unreacted **7c** was recovered in the form of **4**. The difference in the ring size between **7d** and

7e was reflected in the difference in the yield of **1**. Thus, the yield of **1** was higher in the reaction of **7d** than that in **7e**, probably due to the ring strain in five-membered **7d** (entries 4 and 5). The yield of **1** was highest in entry 4. Boronic ester **7f**, a dimethyl analog of **7e**, showed lower reactivity toward **2** due to the steric hindrance by the two methyl groups.

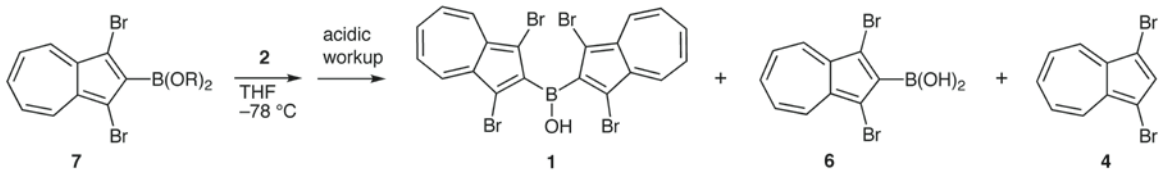

Table 2. Reaction of **7** with **2**

entry	**7**	**2**	time	yield (%)		recovery (%)	
		(equiv)	(h)	**1**	**6**	**4**	**7**
1	**7a**	1.0	1	8	8	32	26
2	**7b**	1.0	1	6	0	71	82
3	**7c**	1.0	1	0	0	68	0
4	**7d**	1.0	1	43	46	46	0
5	**7e**	1.0	1	34	20	24	0
6	**7f**	1.0	1	27	57	56	0

The yields of **1** and **6** are based on **7**.

The recovery of **4** is based on **4** used in the lithiation.

We emphasize that **1** is air stable and can be separated from **6** by silica gel chromatography; in contrast, most diarylborinic acids, especially electron-rich congeners, are unstable and undergo oxidative fragmentation to phenols and phenylboronic acids under ambient conditions.[6,7,10] Considering that electron-rich diarylborinic acids are generally unstable, the azulenyl group of **1** may act as an electron-withdrawing group due to the two bromo substituents, suppressing the oxidative fragmentation. This is suggested by the fact that the ^{1}H NMR spectrum of **1** (DMSO-d_6) featured a specific resonance for the hydroxyl proton in the downfield region at δ 11.06 ppm. The hydroxyl proton of a cyclic diarylborinic acid derived from diphenyl ether resonates more upfield (δ 9.85 ppm) in the same solvent.[6] Alternatively, the four large bromo substituents may effectively protect the boron atom and lead to the kinetic stabilization of **1** against oxidative degradation. In fact, the UV/vis absorption spectrum of **1** (THF) showed a little red shift of the longer wavelength absorption band (λ_{max} = 650 nm) compared to that of **6** (λ_{max} = 623 nm) and the absorbance (ε) in **1** was almost twice as large as that in **6**, suggesting that the interaction between the azulenyl groups through the boron atom is not so efficient.

For long-term storage and convenient separation from boronic acids, borinic acids are generally esterified with ethanolamine or *N*,*N*-dimethylethanolamine.[15] The resulting esters are crystalline and are more

stable than the parent borinic acids owing to the intramolecular boron–nitrogen coordination bond. In order to know how the nonalternant azulenyl ligand affects the structure and reactivities of **1** depending on the change in the valency of the boron center, we examined to apply this reaction to **1**. When we esterified **1** with *N*,*N*-dimethylethanolamine, the reaction took place immediately. However, unlike usual diarylborinic acids, corresponding ester **8** did not form, and the boron–carbon bonds cleaved by protodeboronation[21] to give **4** quantitatively (Scheme 4). These results indicate that the nonalternant azulenyl group stabilizes the structure of **1** but activates that of tetracoordinate borinate **8**. The instability of **8** may be attributed to the strong electron-donation from the tetracoordinate boron to the inherent negatively polarized five-membered ring of the azulenyl group. This makes borinate **8** so nucleophilic compared with parent **1** as to undergo facile protonation at the 2-position giving **4**. The protodeboronation took place when **1** was treated with *t*-BuOK.

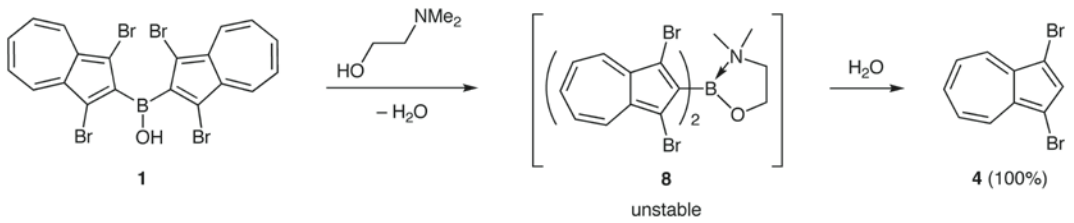

Scheme 4. Reaction of **1** with *N*,*N*-dimethylethanolamine

Diarylborinic acids have recently attracted attention as catalysts for diol activation and glycosylation.[7] A more electron-rich borinic acid would display higher catalytic activity owing to the higher nucleophilicity of its tetracoordinate borinate derivative.[7] Furthermore, the improved stability toward oxidation in air relative to the parent diphenylborinic acid may also be desirable in these catalysts.[7] Our present work shows an example of an air-stable diarylborinic acid that forms a more nucleophilic tetracoordinate borinate than ordinary diarylborinic acids.

NMR spectroscopic study: Table 3 shows the chemical shifts in the ^{13}C, ^{1}H and ^{11}B NMR spectra of **1**. The C1 and C2 signals of **1** exhibited a downfield shift compared with those of **4**. However, the signals of the C3–C6 carbons of **1** showed chemical shifts almost identical to those of **4**. This indicates that the downfield shift is only caused by the inductive effect of the hydroxyboryl group and that π-polarization is not increased in the azulenyl group by introducing the boryl group.

When excess triethylamine was added to the THF-d_8 solution of **1**, the C2 carbon signals underwent a downfield shift, whereas the C3–C6 carbon signals underwent an upfield shift. Furthermore, the signals of the seven-membered ring protons H4–H6 in **1** underwent an upfield shift. The ^{11}B NMR study of **1** revealed that the signal of the boron atom in **1** (δ 44.2 ppm) underwent a considerable upfield shift (δ 4.2

ppm) after addition of triethylamine, indicating the coordination of triethylamine to the boron atom of **1**.

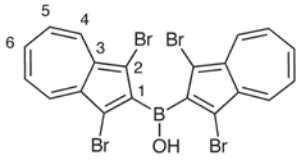

1

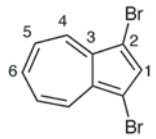

4

Table 3. ^{13}C, ^{1}H and ^{11}B NMR spectral data (ppm) of **1**

	1 (DMSO-d_6)	**4** (DMSO-d_6)	**1** (THF-d_8)	**1** + Et_3N (THF-d_8)
C1	148.6	137.8	–[a]	–[a]
C2	107.4	101.7	109.1	111.1
C3	135.6	135.1	137.3	134.1
C4	136.6	136.7	137.8	137.3
C5	124.7	125.0	125.0	123.4
C6	141.2	141.2	141.5	138.0
H1		8.04		
H4	8.30	8.31	8.23	8.16
H5	7.40	7.45	7.28	7.10
H6	7.83	7.87	7.69	7.46
B	–[a]		44.2	4.2

[a] not observed

These findings clarify the change in the π-polarization of the azulene nucleus accompanied by the change in the geometry of the boron to a tetracoordinate structure (Scheme 5). Namely, the π-polarization of the azulenyl group in **1**•NEt_3 is clearly weakened compared with that of the parent **1**. This tendency is completely different from the results we observed previously in the azulenylpnictogen derivatives, where the π-polarization was increased, *i.e.*, the five-membered ring carbons underwent an upfield shift while the seven-membered ring carbons underwent a downfield shift by changing the pnictogen center from the tricoordinate to the pentacoordinate.[3] It has been reported that the changes in chemical shifts (δc) of anionic pentacoordinate diaryltrifluorosilicates vs the corresponding neutral tetracoordinate diaryldifluorosilanes show the charge distribution in the aryl groups of the silicates (Scheme 5).[22] The charge distribution in the phenyl groups in the silicate is explained by the electron-donating nature by the $SiPhF_3^-$ group via the π-polarization. It is worthy of note here that the charge distribution pattern in the phenyl groups of the silicate, with the positively and negatively polarized carbons at the ortho and meta positions, respectively, is similar to that in the azulenyl groups of **1**•NEt_3. This indicates that the B(azulenyl)(OH)(NEt_3) group has an electron-donating nature. Although we could not get information

about the π-polarization of **8**, the B(azulenyl)($OCH_2CH_2NMe_2$) group of **8** is expected to be more electron-donating than the B(azulenyl)(OH)(NEt_3) group of **1**•NEt_3 since the intramolecular coordination of the nitrogen atom in **8** forms the rigid five-membered chelate ring. This is consistent with the high nucleophilicity of **8**.

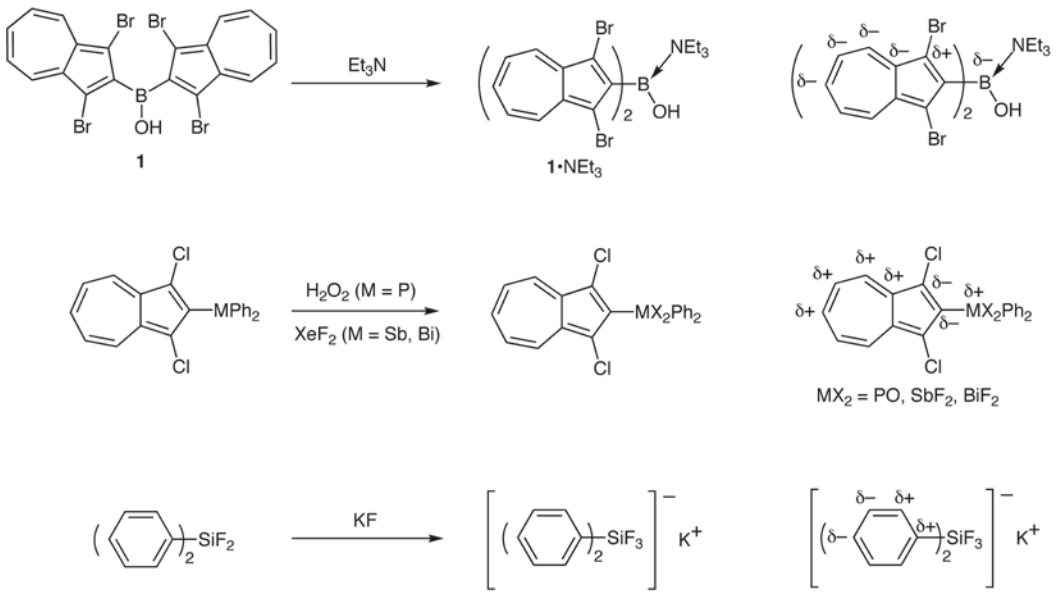

Scheme 5. π-Polarization generated on the aryl ligands

X-Ray crystallographic study: To carry out X-ray structure analysis of **1**, we prepared single crystals of **1**. After many attempts, we found that ethyl acetate is the best solvent. The molecular structure of **1** is shown in Figure 1, and the selected bond lengths, atomic distances and angles are shown in Table 4. The solvent molecule is incorporated in the crystal.

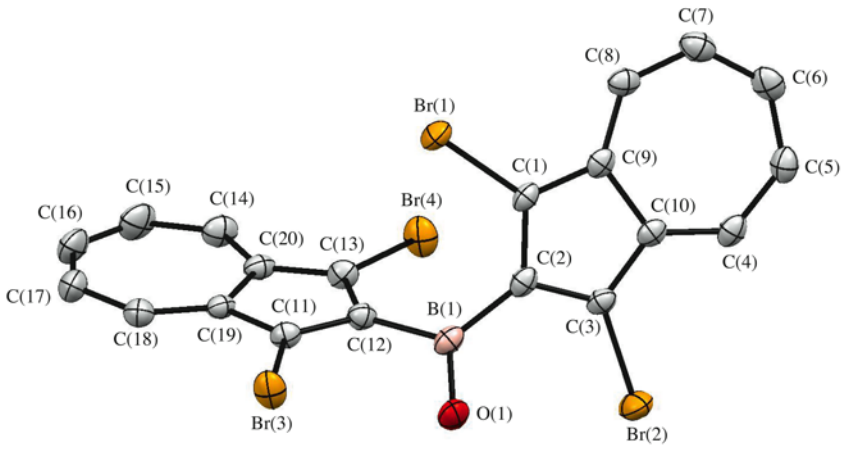

Figure 1. Molecular structure of **1**

Owing to the steric repulsion between the bromine atoms, the two azulenyl groups are twisted with the angles C(11)–C(12)–B(1)–C(2) and C(1)–C(2)–B(1)–C(12) of 133.1(3)° and 144.4(3)°, respectively, which indicates that the vacant 2p-orbital of the B(1) atom does not efficiently conjugate with the azulenyl groups. This is consistent with the finding inferred from the UV/vis spectroscopic study of **1**. The intramolecular B•••Br distances are in the range of 3.433–3.481 Å, which are within the sum of the van der Waals radii[23] of boron and bromine atoms. The four bromo substituents surround the boron atom. Hence, the unique stability of **1** may arise from the kinetic stabilization by these large bromo substituents. Dimesitylborinic acid is air-stable owing to the kinetic stabilization by the bulky mesityl groups and shows polymorphism.[11] The geometry around the boron atom of **1** is similar to that of dimesitylborinic acid, but the boron–oxygen and boron–carbon bonds of **1** are a little shorter than those of dimesitylborinic acid. This indicates that the azulenyl group is more electron-withdrawing than the mesityl group.

Table 4. Selected bond lengths (Å), atomic distances (Å) and angles (°) for **1**

Bond lengths		Torsion angles	
B(1)–O(1)	1.347(5)	C(11)–C(12)–B(1)–C(2)	133.1(3)
B(1)–C(2)	1.573(6)	C(1)–C(2)–B(1)–C(12)	144.4(3)
B(1)–C(12)	1.567(6)	C(1)–C(2)–B(1)–O(1)	–36.9(5)
C(1)–C(2)	1.412(5)	C(13)–C(12)–B(1)–O(1)	136.9(3)
C(2)–C(3)	1.414(5)	B(1)–C(2)–C(3)–Br(2)	0.3(5)
C(3)–C(10)	1.396(5)	C(2)–C(1)–C(9)–C(8)	178.3(3)
C(4)–C(10)	1.384(5)	Intramolecular atomic distances	
C(1)–C(9)	1.408(5)	Br(1)•••B(1)	3.481(4)
C(4)–C(5)	1.390(6)	Br(2)•••B(1)	3.433(4)
C(5)–C(6)	1.383(7)	Br(3)•••B(1)	3.472(4)
C(6)–C(7)	1.390(6)	Br(4)•••B(1)	3.440(4)
C(7)–C(8)	1.390(6)	Intermolecular atomic distances	
C(8)–C(9)	1.384(6)	O(1)•••O(3)	2.786(4)
C(9)–C(10)	1.497(5)	O(2)•••O(2)	3.030(4)
Bond angles		C(11)•••C(26)	3.403(5)
O(1)–B(1)–C(2)	114.7(4)	C(16)•••C(23)	3.428(5)
O(1)–B(1)–C(12)	123.0(3)	C(18)•••C(28)	3.460(5)
C(2)–B(1)–C(12)	122.3(3)	C(19)•••C(26)	3.482(5)
C(1)–C(2)–C(3)	105.1(3)	C(20)•••C(25)	3.419(5)

Two types of borinic acid molecules, B(1) and B(2), each bearing a boron atom are present in the crystal (Figure 2). The B(1) molecule interacts with an ethyl acetate molecule by hydrogen bonding between the O(1) atom and the carbonyl oxygen atom O(3). The B(2) molecule forms a dimeric structure with another B(2) molecule by hydrogen bonding between the O(2) atoms. One of the azulenyl groups of the B(1) molecule forms head-to-tail π–π stacking with one of the azulenyl groups of the B(2) molecule, with the shortest interatomic distance of 3.403(5) Å between the C(11) and C(26) atoms.

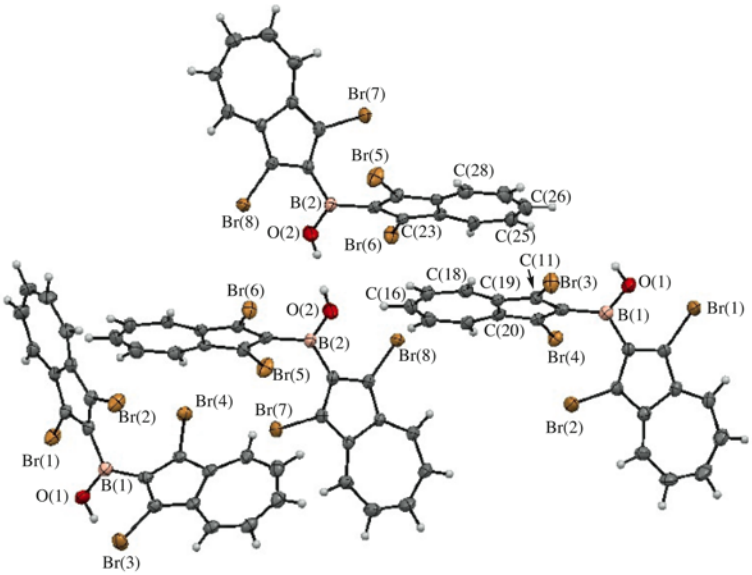

Figure 2. Intermolecular interaction of **1**. An ethyl acetate molecule is omitted for clarity.

CONCLUSION

We obtained diazulenylborinic acid **1** and characterized the structure by X-ray structure analysis. Furthermore, we revealed the change in the π-polarization of **1** by the change in the geometry of the boron from the tricoordinate to the tetracoordinate structure. The mode of the induced π-polarization in the Et_3N•**1** complex was completely reversed compared with our previously reported azulenylpnictogens. These findings indicate that the unique π-electron system of nonalternant azulene has high polarizability and low aromatic resonance energy.

EXPERIMENTAL

All reactions were carried out under argon, unless otherwise noted. THF was distilled from sodium benzophenone ketyl under argon before use. ^{1}H and ^{13}C NMR spectra were recorded in $CDCl_3$ or DMSO-d_6 on a Bruker Avance III-400 (400 MHz) spectrometer with tetramethylsilane as an internal standard. ^{11}B NMR spectra were measured in $CDCl_3$ or THF-d_8 on a Bruker Avance III-400 spectrometer at 128 MHz with proton decoupling relative to boron trifluoride diethyl etherate as the external reference. IR spectra were recorded as KBr pellets on a Nicolet FT-IR Impact 410 spectrophotometer. UV/vis

spectra were measured in THF by means of a Shimadzu UV-1600PC spectrophotometer. HRMS were recorded on a Bruker Daltonics micrOTOF II (APCI) instrument. Charts of ^{1}H, ^{13}C, and ^{11}B NMR spectra of reported compounds are summarized in Supporting Information.

1,3-Dibromoazulen-2-ylboronic Acid (6): To a stirred solution of lithium 2,2,6,6-tetramethylpiperidide (ca. 18 mmol) prepared from 2,2,6,6-tetramethylpiperidine (3.04 mL, 18 mmol) and butyllithium (18 mmol) in THF (40 mL) at –78 °C was added a solution of **4** (3.43 g, 12 mmol) in THF (40 mL) at the same temperature. The color of the solution immediately turned from blue to dark green, showing the generation of **2**. To this solution thus obtained was added trimethyl borate (1.6 mL, 14.4 mmol), and the resulting mixture was stirred for 2 h, during which time the temperature was raised to ambient. The reaction was quenched with brine (50 mL), and a 10% aqueous solution of HCl (1 mL) was added. The resulting mixture was extracted with EtOAc (50 mL × 3). The combined extracts were concentrated to leave an oily residue, which was purified by chromatography on a silica gel column with hexane–EtOAc (5:1) to give **6** (3.17 g, 80%). Green solid; mp 123–125 °C; IR 3330, 1574, 1473, 1456, 1388, 1343, 1325, 1271, 1220 cm^{-1}; ^{1}H NMR (400 MHz, DMSO-d_6) δ 7.42 (t, J = 10.0 Hz, 2H), 7.82 (t, J = 10.0 Hz, 1H), 8.27 (d, J = 9.6 Hz, 2H), 8.71 (s, 2H); ^{13}C NMR (100 MHz, DMSO-d_6) δ 105.4, 124.6, 135.3, 135.8, 140.5. One ipso carbon could not be assigned due to weak signal response; ^{11}B NMR (128 MHz, DMSO-d_6) δ 29.2. UV/vis (THF) λ_{max}/nm (ε) 356 (5428), 372 (3846), 623 (374). HRMS (APCI) (Br-79): *m/z* $[M+H]^+$ calcd for $C_{10}H_8BBr_2O_2$: 328.8984; found: 328.8979.

1,3-Dibromoazulen-2-ylboronic Acid Ester (7): To a solution of **6** (495 mg, 1.5 mmol) in THF (1.5 mL) containing 3A molecular sieves was added diol (1.5 mmol) at room temperature. The resulting mixture was stirred for 3 h at the same temperature. After filtration, the filtrate was concentrated to leave an oily residue, which was recrystallized from hexane to give **7**.

1,3-Dibromoazulen-2-ylboronic Acid Pinacol Ester (7a): green solid; yield 88%; mp 138–140 °C; IR 2976, 1576, 1480, 1492, 1247, 1141 cm^{-1}; ^{1}H NMR (400 MHz, $CDCl_3$) δ 1.47 (s, 12H), 7.19 (t, J = 9.6 Hz, 2H), 7.61 (t, J = 9.6 Hz, 1H), 8.76 (d, J = 9.6 Hz, 2H); ^{13}C NMR (100 MHz, $CDCl_3$) δ 25.0, 84.9, 108.6, 124.1, 136.4, 137.5, 140.8. One ipso carbon could not be assigned due to weak signal response; ^{11}B NMR (128 MHz, $CDCl_3$) δ 30.4. HRMS (APCI) (Br-79): *m/z* $[M+H]^+$ calcd for $C_{16}H_{18}BBr_2O_2$: 410.9767; found: 410.9761.

1,3-Dibromoazulen-2-ylboronic Acid Catechol Ester (7b): green solid; yield 89%; mp 233–235 °C; IR 1576, 1466, 1390, 1350, 1330, 1252, 1240 cm^{-1}; ^{1}H NMR (400 MHz, $CDCl_3$) δ 7.19–7.21 (m, 2H), 7.28 (t, J = 9.6 Hz, 2H), 7.44–7.46 (m, 2H), 7.70 (t, J = 10.0 Hz, 1H), 8.44 (d, J = 9.6 Hz, 2H); ^{13}C NMR (100 MHz, $CDCl_3$) δ 110.4, 113.2, 123.3, 124.7, 137.0, 139.2, 142.2, 148.4. One ipso carbon could not be assigned due to weak signal response; ^{11}B NMR (128 MHz, $CDCl_3$) δ 30.7. HRMS (APCI) (Br-79): *m/z*

$[M+H]^+$ calcd for $C_{16}H_{10}BBr_2O_2$: 402.9141; found: 402.9135.

1,3-Dibromoazulen-2-ylboronic Acid *N*-Methyldiethanolamine Ester (7c): green solid; yield 100%; mp 127–129 °C; IR 1570, 1456, 1388, 1340, 1246, 1113, 1036 cm^{-1}; ^1H NMR (400 MHz, $CDCl_3$) δ 2.42 (s, 3H), 3.18–3.29 (m, 4H), 4.19–4.25 (m, 2H), 4.31–4.37 (m, 2H), 7.17 (t, *J* = 10.0 Hz, 2H), 7.55 (t, *J* = 10.0 Hz, 1H), 8.46 (d, *J* = 9.6 Hz, 2H); ^{13}C NMR (100 MHz, $CDCl_3$) δ 46.1, 60.9, 62.4, 110.9, 123.5, 135.9, 136.9, 139.1. One ipso carbon could not be assigned due to weak signal response; ^{11}B NMR (128 MHz, $CDCl_3$) δ 11.4. HRMS (APCI) (Br-79): *m/z* $[M+H]^+$ calcd for $C_{15}H_{17}BBr_2NO_2$: 411.9719; found: 411.9714.

1,3-Dibromoazulen-2-ylboronic Acid Ethylene Glycol Ester (7d): green solid; yield 89%; mp 141–143 °C; IR 1580, 1480, 1400, 1350, 1330, 1270, 1240, 1020 cm^{-1}; ^1H NMR (400 MHz, $CDCl_3$) δ 4.53 (s, 4H), 7.22 (t, *J* = 10.0 Hz, 2H), 7.63 (t, *J* = 10.0 Hz, 1H), 8.36 (d, *J* = 9.2 Hz, 2H); ^{13}C NMR (100 MHz, $CDCl_3$) δ 66.4, 109.9, 124.3, 136.7, 138.5, 141.5. One ipso carbon could not be assigned due to weak signal response; ^{11}B NMR (128 MHz, $CDCl_3$) δ 30.5. HRMS (APCI) (Br-79): *m/z* $[M+H]^+$ calcd for $C_{12}H_{10}BBr_2O_2$: 354.9141; found: 354.9135.

1,3-Dibromoazulen-2-ylboronic Acid 1,3-Propanediol Ester (7e): green solid; yield 99%; mp 121–123 °C; IR 1576, 1481, 1431, 1323, 1281, 1252, 1236 cm^{-1}; ^1H NMR (400 MHz, $CDCl_3$) δ 2.19 (quin, *J* = 5.6 Hz, 2H), 4.29 (t, *J* = 5.6 Hz, 4H), 7.21 (t, *J* = 10.0 Hz, 2H), 7.61 (t, *J* = 10.0 Hz, 1H), 8.30 (d, *J* = 10.0 Hz, 2H); ^{13}C NMR (100 MHz, $CDCl_3$) δ 27.7, 62.6, 108.1, 124.0, 136.5, 137.2, 140.3. One ipso carbon could not be assigned due to weak signal response; ^{11}B NMR (128 MHz, $CDCl_3$) δ 27.2. HRMS (APCI) (Br-79): *m/z* $[M+H]^+$ calcd for $C_{13}H_{12}BBr_2O_2$: 368.9297; found: 368.9292.

1,3-Dibromoazulen-2-ylboronic Acid 2,2-Dimethyl-1,3-propanediol Ester (7f): a blue solid; yield 93%; mp 74–76 °C; IR 1577, 1477, 1421, 1327, 1254, 1238, 1200 cm^{-1}; ^1H NMR (400 MHz, $CDCl_3$) δ 1.16 (s, 6H), 3.90 (s, 4H), 7.21 (t, *J* = 10.0 Hz, 2H), 7.61 (t, *J* = 10.0 Hz, 1H), 8.29 (d, *J* = 9.6 Hz, 2H); ^{13}C NMR (100 MHz, $CDCl_3$) δ 22.1, 32.1, 72.9, 108.0, 124.0, 136.5, 137.2, 140.3. One ipso carbon could not be assigned due to weak signal response; ^{11}B NMR (128 MHz, $CDCl_3$) δ 27.1. HRMS (APCI) (Br-79): *m/z* $[M+H]^+$ calcd for $C_{15}H_{16}BBr_2O_2$: 396.9610; found: 396.9605.

Bis(1,3-dibromoazulen-2-yl)borinic Acid (1): To a stirred solution of lithium 2,2,6,6-tetramethylpiperidide (ca. 3 mmol) prepared from 2,2,6,6-tetramethylpiperidine (0.51 mL, 3 mmol) and butyllithium (3 mmol) in THF (4 mL) at –78 °C was added a solution of **4** (572 mg, 2 mmol) in THF (40 mL) at the same temperature. The color of the solution immediately turned from blue to dark green, showing the generation of **2**. To this solution thus obtained was added **7d** (712 mg, 2 mmol) in THF (4 mL), and the resulting mixture was stirred for 2 h, during which time the temperature was raised to ambient. The reaction was quenched with brine (50 mL), and the resulting mixture was extracted with

EtOAc (50 mL × 3). The combined extracts were concentrated to leave an oily residue, which was purified by chromatography on a silica gel column with hexane–EtOAc (10:1) to give **1** (550 mg, 46%). Green solid; mp 185–190 °C (decomp); IR 3546, 1575, 1456, 1390, 1344, 1321, 1256, 1140, 1018 cm^{-1}; ^1H NMR (400 MHz, DMSO-d_6) δ 7.40 (t, J = 10.0 Hz, 4H), 7.83 (t, J = 10.0 Hz, 2H), 8.30 (d, J = 10.0 Hz, 4H), 11.06 (s, 1H); ^{13}C NMR (100 MHz, DMSO-d_6) δ 107.4, 124.7, 135.6, 136.6, 141.2, 148.6; ^{11}B NMR (128 MHz, THF-d_8) δ 44.2. UV/vis (THF) λ_{max}/nm (ε) 358 (10198), 371 (sh, 5659), 650 (830). HRMS (APCI) (Br-79): *m/z* $[M–H]^-$ calcd for $C_{20}H_{10}BBr_4O$: 592.7558; found: 592.7564.

X-Ray crystallographic study: A green prismatic crystal **1**bfwas mounted on a glass fiber. All measurements were made with a Rigaku Mercury 70 diffractometer using graphite monochromated Mo-Kα radiation. The data were collected at a temperature of –119 ± 1 °C to a maximum 2θ value of 55.0°. The structure was solved by direct methods[24] and expanded using Fourier techniques. The non-hydrogen atoms were refined anisotropically. The removal of solvents by PLATON/SQUEEZE could slightly improve the refinement (R = 0.0386 and Rw = 0.1002, GOF = 1.105), but disordered EtOAc molecules were assigned in the present report (electron count = 435/cell from PLATON/SQUEEZE; 384 electrons for $8CH_3COOC_2H_5$/cell). All calculations were performed using the CrystalStructure[25] crystallographic software package except for refinement, which was performed using SHELXL97.[26] Crystal data, data collection summary and refinement parameters of **1** are given in Supporting Information. Deposition number CCDC-1534423 for compound **1**. Free copies of the data can be obtained via http://www.ccdc.cam.ac.uk/conts/retrieving.html (or from the Cambridge Crystallographic Data Centre, 12 Union Road, Cambridge, CB2 1EZ, UK; Fax: +44 1223 336033; e-mail: deposit@ccdc.cam.ac.uk).

ACKNOWLEDGEMENTS

This work was supported by JSPS KAKENHI Grant Number 16K05697 to T. M. We are grateful to the Center of Instrumental Analysis, Yamaguchi University.

REFERENCES

1. (a) T. Shoji, A. Maruyama, M. Tanaka, D. Nagai, E. Shimomura, K. Fujimori, S. Ito, T. Okujima, K. Toyota, and M. Yasunami, *ChemistrySelect*, 2016, **1**, 49; (b) T. Shoji, A. Maruyama, T. Araki, S. Ito, and T. Okujima, *Org. Biomol. Chem.*, 2015, **13**, 10191; (c) S. Ito, S. Yamazaki, S. Kudo, R. Sekiguchi, J. Kawakami, M. Takahashi, T. Matsuhashi, K. Toyota, and N. Morita, *Tetrahedron*, 2014, **70**, 2796; (d) H. Nakagawa, S. Tsukada, N. Abe, and T. Gunji, *Heteroat. Chem.,* 2014, **25**, 389.
2. Y. Sugihara, T. Murafuji, N. Abe, M. Takeda, and A. Kakehi, *New J. Chem.,* 1998, 1031.

3. (a) A. F. M. Mustafizur Rahman, T. Murafuji, T. Shibasaki, K. Suetake, K. Kurotobi, Y. Sugihara, N. Azuma, and Y. Mikata, *Organometallics*, 2007, **26**, 2971; (b) A. F. M. Mustafizur Rahman, T. Murafuji, K. Kurotobi, Y. Sugihara, and N. Azuma, *Organometallics*, 2004, **23**, 6176.
4. (a) M. J. Białek, N. Sprutta, and L. Grażyński, *Inorg. Chem.*, 2016, **55**, 12061; (b) J. Kuwabara, G. Munezawa, K. Okamoto, and T. Kanbara, *Dalton Trans.*, 2010, **39**, 6255; (c) R. E. Robinson, T. C. Holovics, S. F. Deplazes, D. R. Powell, G. H. Lushington, W. H. Thompson, and M. V. Barybin, *Organometallics*, 2005, **24**, 2386; (d) A. J. Arce, Y. De Sanctis, E. Galarza, M. T. Garland, R. Gobetto, R. Machado, J. Manzur, A. Russo, E. Spodine, and M. J. Stchedroff, *Organometallics*, 2001, **20**, 359.
5. (a) D. Donghi, D. Maggioni, T. Beringhelli, G. D'Alfonso, P. Mercandelli, and A. Sironi, *Eur. J. Inorg. Chem.*, 2008, 1645; (b) T. Beringhelli, G. D'Alfonso, D. Donghi, D. Maggioni, P. Mercandelli, and A. Sironi, *Organometallics*, 2007, **26**, 2088; (c) G. J. P. Britovsek, J. Ugolotti, P. Hunt, and A. J. P. White, *Chem. Commun.*, 2006, 1295.
6. E. Dimitrijević, M. Cusimano, and M. S. Taylor, *Org. Biomol. Chem.*, 2014, **12**, 1391.
7. E. Dimitrijević and M. S. Taylor, *Chem. Sci.*, 2013, **4**, 3298.
8. T. Mohy El Dine, D. Evans, J. Rouden, and J. Blanchet, *Chem. Eur. J.*, 2016, **22**, 5894.
9. A. Nasr, P.-A. R. Breuil, D. C. Silva, M. Berthod, N. Dellus, E. Jeanneau, M. Lemaire, and H. Olivier-Bourbigou, *Organometallics,* 2013, **32**, 5320.
10. G. N. Chremos, H. Weidmann, and H. K. Zimmerman, *J. Org. Chem.*, 1961, **26**, 1683.
11. (a) M. Kuhlmann, T. Baumgartner, and M. Parvez, *Acta Cryst.*, 2008, **E64**, o1185; (b) C. D. Entwistle, A. S. Batsanov, and T. B. Marder, *Acta Cryst.*, 2007, **E63**, o2639.
12. S. Luliński and J. Serwatowski, *Acta Cryst.*, 2010, **E66**, o1711.
13. S. M. Cornet, K. B. Dillon, C. D. Entwistle, M. A. Fox, A. E. Goeta, H. P. Goodwin, T. B. Marder, and A. L. Thompson, *Dalton Trans.*, 2003, 4395.
14. T. Beringhelli, G. D'Alfonso, D. Donghi, D. Maggioni, P. Mercandelli, and A. Sironi, *Organometallics*, 2003, **22**, 1588.
15. S. J. Rettig and J. Trotter, *Can. J. Chem.*, 1983, **61**, 2334.
16. (a) L. Marciasini, B. Cacciuttolo, M. Vaultier, and M. Pucheault, *Org. Lett.*, 2015, **17**, 3532; (b) D. D. Winkle and K. M. Schaab, *Org. Process Res. Dev.*, 2001, **5**, 450.
17. K. Kurotobi, H. Tabata, M. Miyauchi, A. F. M. Mustafizur Rahman, K. Migita, T. Murafuji, Y. Sugihara, H. Shimoyama, and K. Fujimori, *Synthesis*, 2003, 30.
18. A. Hofer, G. Kovacs, A. Zappatini, M. Leuenberger, M. A. Hediger, and M. Lochner, *Bioorg. Med. Chem. Lett.*, 2013, **21**, 3202.
19. C. D. Roy and H. C. Brown, *J. Organomet. Chem.*, 2007, **692**, 784.

20. T. Murafuji, K. Sugimoto, S. Yanagimoto, T. Moriya, Y. Sugihara, Y. Mikata, M. Kato, and S. Yano, *Heterocycles*, 2001, **54**, 929.
21. (a) P. A. Cox, A. G. Leach, A. D. Campbell, and G. C. Lloyd-Jones, *J. Am. Chem. Soc.*, 2016, **138**, 9145; (b) D. Donghi, D. Maggioni, T. Beringhelli, and G. D'Alfonso, *Eur. J. Inorg. Chem.*, 2008, 3606.
22. K. Tamao, T. Hayashi, Y. Ito, and M. Shiro, *Organometallics*, 1992, **11**, 182.
23. M. Mantina, A. C. Chamberlin, R. Valero, C. J. Cramer, and D. G. Truhlar, *J. Phys. Chem. A*, 2009, **113**, 5806.
24. SIR92: A. Altomare, G. Cascarano, C. Giacovazzo, and A. Guagliardi, *J. Appl. Cryst*., 1993, **26**, 343.
25. CrystalStructure 4.1: Crystal Structure Analysis Package; Rigaku Corporation (2000-2014), Tokyo 196-8666, Japan.
26. SHELXL97: G. M. Sheldrick, *Acta Cryst*., 2008, **A64**, 112.